Mol Neurobiol (2018) 55:1123–1135
DOI 10.1007/s12035-017-0386-9

IGF-1R Regulates the Extracellular Level of Active MMP-2, Pathological Neovascularization, and Functionality in Retinas of OIR Mouse Model

Valeria E. Lorenc[1,2] · Paula V. Subirada Caldarone[1] · María C. Paz[1] · Darío G. Ferrer[1] · José D. Luna[3] · Gustavo A. Chiabrando[1] · María C. Sánchez[1]

Received: 4 October 2016 / Accepted: 4 January 2017 / Published online: 17 January 2017

Abstract In ischemic proliferative diseases such as retinopathies, persistent hypoxia leads to the release of numerous neovascular factors that participate in the formation of abnormal vessels and eventually cause blindness. The upregulation and activation of metalloproteinases (MMP-2 and MMP-9) represent a final common pathway in this process. Although many regulators of the neovascular process have been identified, the complete role of the insulin-like growth factor 1 (IGF-1) and its receptor (IGF-1R) appears to be significantly more complex. In this study, we used an oxygen-induced retinopathy (OIR) mouse model as well as an in vitro model of hypoxia to study the role of MMP-2 derived from Müller glial cells (MGCs) and its relation with the IGF-1/IGF-1R system. We demonstrated that MMP-2 protein expression increased in P17 OIR mice, which coincided with the active phase of the neovascular process. Also, glutamine synthetase (GS)-positive cells were also positive for MMP-2, whereas IGF-1R was expressed by GFAP-positive cells, indicating that both proteins were expressed in MGCs. In addition, in the OIR model a single intravitreal injection of the IGF-1R blocking antibody (αIR3) administered at P12 effectively prevented pathologic neovascularization, accelerated physiological revascularization, and improved retinal functionality at P17. Finally, in MGC supernatants, the blocking antibody abolished the IGF-1 effect on active MMP-2 under normoxic and hypoxic conditions without affecting the extracellular levels of pro-MMP-2. These results demonstrate, for the first time, that the IGF-1/IGF-1R system regulates active MMP-2 levels in MGCs, thus contributing to MEC remodeling during the retinal neovascular process.

Keywords Müller glial cell · Matrix metalloproteinases · IGF-1R · Hypoxia · Oxygen-induced retinopathy · IGF-1R blocking antibody αIR3

Introduction

Abnormal blood vessel growth—so-called neovascularization (NV)—in the retina is a hallmark of many retinal diseases, such as retinopathy of prematurity (ROP) and proliferative diabetic retinopathy [1]. These pathological conditions occur as a result of hypoxic insults to the retina which stimulate the release of numerous neovascular factors [2, 3]; among them, the vascular endothelial growth factor (VEGF) is rightfully considered a master switch for angiogenesis [4]. In the presence of low IGF-1 levels, however, VEGF is insufficient to promote vigorous retinal angiogenesis [5, 6], which indicates that the IGF-1/IGF-1R system is necessary to promote the maximum function of VEGF [7]. In this way, it has been shown that vessel-specific knockout of IGF-1 receptors protects from retinal NV in a mouse model of oxygen-induced retinopathy (OIR) [8], thereby highlighting the importance of IGF-1 signaling in the endothelium. Though IGF-1R mRNA is present in endothelial cells, it showed a more extensive

Electronic supplementary material The online version of this article (doi:10.1007/s12035-017-0386-9) contains supplementary material, which is available to authorized users.

✉ María C. Sánchez
csanchez@fcq.unc.edu.ar

[1] Centro de Investigaciones en Bioquímica Clínica e Inmunología (CIBICI-CONICET), Departamento de Bioquímica Clínica, Facultad de Ciencias Químicas, Universidad Nacional de Córdoba, Córdoba, Argentina

[2] Present address: The Wilmer Eye Institute, Johns Hopkins University, Baltimore, MD, USA

[3] Centro Privado de Ojos Romagosa-Fundación VER, Córdoba, Argentina

distribution in rat neural retina and predominance in mouse photoreceptors [9, 10]. Thus, the complete role of the IGF-1/IGF-1R system in retinopathies appears to be significantly more complex and indirect due to the effect that this system may have on cells other than the endothelium.

Extracellular matrix (ECM) proteolysis has been considered as one of the first and most sustained activities involved in pathological NV [11]. Also in the retina, proteolysis by matrix metalloproteinases (MMPs)—zinc-dependent endopeptidases that degrade various components of the ECM—has been reported to play an important role in several retinopathies [12, 13]. Despite well-designed studies aimed at improving our understanding of the role of these proteases in eye diseases, contradictory results from several investigations have made it difficult to determine the different cell contribution of MMPs to ocular NV. By using an in vitro model, we have recently demonstrated that IGF-1 regulates the extracellular level of active MMP-2 secreted by MGCs and that it promotes cell motility in a process involving the activation of IGF-1R and PI3K signaling pathway [14]. In this study, we sought to contribute to further the understanding of the MGC-derived MMP-2 role in a mouse model of OIR and its relation with the IGF-1/IGF-1R system within the retinal environment, with the purpose of identifying potential targets for the treatment of retinopathies.

Materials and Methods

Reagents

Recombinant human IGF-1 was purchased from Sigma-Aldrich, St. Louis, MO. Immunoblots of retinal extracts and cell lysates were performed with the following primary antibodies: mouse monoclonal anti-IGF-1R, rabbit polyclonal anti-calreticulin, rabbit polyclonal anti-MMP-2, and mouse monoclonal MT1-MMP antibodies, which were all from Abcam, Inc. (Cambridge, MA, USA), and mouse monoclonal anti-HIF-1 from BD Biosciences (San Jose, CA, USA). Dilutions for primary antibodies were between 1/250 and 1/1000, whereas for secondary antibodies, they were 1/5000. Secondary antibodies used for immunoblotting were horseradish peroxidase–conjugated streptavidin (Thermo Fisher Scientific, Rockford, IL, USA). For immunohistochemistry, we used the same anti-IGF-1R and anti-MMP-2 as in Western blot assays, a rabbit polyclonal anti-glial fibrillary acidic protein (GFAP) (Dako, Carpinteria, CA) and a mouse monoclonal anti-glutamine synthetase (GS) obtained from Millipore Corporation (MA, USA). Secondary antibodies were raised in goat against rabbit or mouse IgG conjugated with Alexa Fluor 488 and 594, respectively (Molecular Probes, Eugene, OR, USA). Dilutions for primary antibodies were between 1/50 and 1/100, whereas for secondary antibodies, they were 1/800. For whole mount staining, Alexa Fluor 488 isolectin GS-IB4 conjugate from Molecular Probes, Inc. (Eugene, OR, USA) was used. In some experiments, a mouse monoclonal antibody specific against the IGF-1 receptor, αIR3 (Calbiochem, San Diego, CA, USA), was also used to block IGF-1/IGF-1R binding.

Animals

The C57BL/6J mice were treated according to the guidelines of the ARVO Statement for the Use of Animals in Ophthalmic and Vision Research; the experimental procedures were designed and approved by the Institutional Animal Care and Use Committee (CICUAL) of the School of Chemical Sciences, National University of Cordoba (Res. H.C.D. 451/07). All efforts were made to reduce the number of animals used.

Oxygen-Induced Retinopathy in a Mouse Model

In a typical model of OIR [15], litters of mice pups with their nursing mothers were exposed in an infant incubator to high oxygen concentration (75% ± 2%) between postnatal day 7 (P7) and P12. The animals were kept in clear plastic cages with standard light cycles (12 h light/12 h dark). The oxygen was checked twice daily with an oxygen analyzer (Teledyne Analytical Instruments, CA, USA). The hyperoxia treatment caused vaso-obliteration, but retinal development persisted and resulted in a relative retinal hypoxia when the mice were returned to room air (RA) at P12. During the relative hypoxic period, the animals developed extensive retinal NV (peak was reached at P17), underwent MGC activation, neuronal apoptosis and, shortly after P17, NV regression. The mice were sacrificed at various times after the hyperoxia treatment, and their retinas were collected and processed for Western blot, immunohistochemistry, and whole mount assays. Age-matched control C57BL/6 mice were kept in normoxic (RA) conditions. At least three mice per group were used for each of the survival times examined. The data were collected from both males and females, and the results were combined, considering there was no apparent difference between the sexes.

Preparation and Administration of αIR3

The αIR3 (Calbiochem, San Diego, CA, USA) solution was freshly prepared as 100 μg/mL in PBS pH 7.4. After anesthesia with 3% isoflurane, one drop of 0.5% proparacaine hydrochloride ophthalmic solution was applied as a topical anesthetic before intravitreal injection. The eye was punctured at the upper nasal limbus, and a single dose of 1 μL of blocking antibody αIR3 or nonspecific IgG was injected into one eye of each mouse as it was previously described [16]. All mice were sacrificed at P17.

Electroretinography

Electroretinographic activity was assessed at P17 in OIR mice with or without αIR3 treatment. Briefly, after overnight dark adaptation, the mice were anesthetized under dim red illumination, the pupils were dilated with 1% tropicamide (Midril, Alcon, Buenos Aires, Argentina), and the cornea was lubricated with gel drops of 0.4% polietilenglicol 400 and 0.3% propilenglicol (Systane, Alcon, Buenos Aires, Argentina) to prevent corneal damage. The mice were exposed to the stimulus at a distance of 20 cm. A reference electrode was inserted on the back between the ears, a grounding electrode was attached to the tail, and a gold electrode was placed in contact with the central cornea. A dim red light was used to enable accurate electrode placement. The ERGs were simultaneously recorded from both eyes and ten responses to flashes of unattenuated white light (5 cd.s/m^2, 0.2 Hz) from a photic stimulator (light-emitting diodes) set at maximum brightness were amplified, filtered (1.5-Hz low-pass filter, 1000 high-pass filter, notch activated), and averaged (Akonic BIO-PC, Argentina).

The a-wave was measured as the difference in amplitude between the recording at onset and trough of the negative deflection, and the b-wave amplitude was measured from the trough of the a-wave to the peak of the b-wave. The implicit times of the a- and b-waves were measured from the time of flash presentation to the trough of the a-wave or the peak of the b-wave, respectively. Responses were averaged across the two eyes for each mouse in RA condition whereas in OIR eyes treated or not with αIR3 blocking antibody, the retinal responses were individually analyzed.

Retina Whole Mount Immunostaining

The mice were euthanized at P17, and their eyes were enucleated and fixed with freshly prepared 2% paraformaldehyde (PFA) for 1 h. The corneas were removed with scissors along the limbus, and then, the intact retinas were dissected. The retinas were blocked and permeabilized in phosphate-buffered saline (PBS) containing 5% BSA and 1% Triton-X-100 overnight at 4 °C. Then, they were incubated with Alexa Fluor 488-conjugated GSA-IB4 and a rabbit polyclonal MMP-2 antibody. Some whole mount retinas were also incubated with a mouse monoclonal GS antibody. The retinas were then washed with PBS and examined using a confocal laser-scanning microscope (Olympus FluoView FV1200; Olympus Corp., New York, NY, USA) to a ×10 magnification.

Cryosection Preparation and Retinal Protein Extraction

For section preparation, some eyes were enucleated and fixed overnight with 4% PFA. Then, they were incubated in 10% (2 h), 20% (2 h), and 30% sucrose/PBS overnight at 4 °C, and they were placed in a small amount of optimal cutting temperature (OCT) compound (Crioplast, Biopack, Buenos Aires, Argentina) on plastic stubs. Serial sections (of 8-μm thick) were obtained by using a cryostat as we previously described [17], and then stored under dry conditions until immunohistochemical analysis.

For Western blot and zymographic analysis, neural retinas were dissected from RPE/choroid layers and washed. The extracted tissues were homogenized with lysis buffer containing 0.0625 M Tris, pH 6.8, 12.5% glycerol, and 1.25% sodium dodecyl sulfate (SDS) with 1 mM phenylmethylsulfonyl fluoride (PMSF) and protease inhibitor cocktail without metal chelators (Sigma-Aldrich, St. Louis, MO) [18]; and they were stored at −80 °C until used.

Exposure of MIO-M1 Cell Line to IGF-1 Under Normoxic and Hypoxic Conditions

For normoxic and hypoxic assays, we used a spontaneously immortalized human MGC line (MIO-M1) [19] kindly provided by Dr. G. Astrid Limb (UCL, Institute of Ophthalmology and Moorfields Eye Hospital, London, UK). Cells were exposed to normoxia (21% O_2) in a conventional cell incubator with gas mixtures consisting of 74% N_2 and 5% CO_2 or to hypoxia (1,3% O_2) in a Modular Incubator Chamber (Billups-Rothenberg Inc., San Diego, CA, USA) with 93.7% N_2 and 5% CO_2. Under both conditions, the cells were stimulated for 8 h with IGF-1. In some experiments, the cells were pretreated with αIR3 (16 nM) to block IGF-1/IGF-1R binding. At the end of each treatment, cell supernatants were collected whereas cells were harvested in lysis buffer for Western blot analysis. Six identical culture cell dishes were prepared; three were placed under normoxia and the other three under hypoxic conditions.

Immunofluorescence Labeling

To detect IGF1-R in combination with GFAP or MMP-2 in combination with GS, mice cryosections were washed in PBS, blocked with 2% BSA in PBS containing 0.3% Triton-X-100, for 1 h and then incubated with primary antibodies overnight at 4 °C. After the sections were washed with PBS, secondary antibodies against rabbit or mouse IgG conjugated with Alexa Fluor 488 and 594 were applied for 1 h at RT. The sections were also counterstained with Hoechst 33258 (1:30,000 dilution; Molecular Probes) for 7 min. After a thorough rinse, the sections were mounted with FluorSave (Calbiochem, La Jolla, CA) and coverslipped. Negative controls without primary antibody incubation were performed to avoid unspecific signals. The labeling was visualized using a confocal laser-scanning microscope (Olympus FluoView FV1000). Finally, the images were processed with microscope software Viewer Fluoview 4.0 software (Olympus) and Image J 1.40 software (National Institutes of Health, Bethesda, MD, USA).

Western Blot Assay

Protein concentration of retinal extracts and cell lysates was determined by a BCA kit (Pierce, Buenos Aires, Argentina), and 10 mg of proteins was electrophoresed in 10% SDS-PAGE. Then, the proteins were transferred to nitrocellulose membranes (Amersham Hybond ECL; GE Healthcare Bio-Sciences AB, Uppsala, Sweden). Nonspecific binding was blocked with 1% bovine serum albumin (BSA) in Tris-buffer containing 0.01% Tween-20, and the same solution was used to prepare primary antibody dilutions, which were incubated with the membranes at 4 °C overnight. The membranes were incubated with a horseradish peroxidase-conjugated streptavidin secondary antibody for 1 h at room temperature (RT). Antibody detection was performed with enhanced chemiluminescence (Thermo Fisher Scientific) and quantified by densitometric analysis using analysis software (Gel Pro Analyzer; MediaCybernetics, Inc., Rockville, MD, USA).

Gelatin Zymography Assays

The MMP enzymatic (gelatinase) activity in retinal extracts or MIO-M1 cell supernatants were analyzed by zymography assays as previously described [17, 18, 20]. For this purpose, supernatants of cells stimulated with 10 nM IGF-1 (8 h) under normoxic or hypoxic conditions in the presence or absence of blocking antibody αIR3 were collected and stored at −80 °C until used. Then, the cell supernatants or retinal extracts were resolved on 10% SDS-PAGE/1.5% gelatin (Sigma-Aldrich, St. Louis, MO) under denaturing and nonreducing conditions. The gels were soaked for 1 h with 2.5% Triton X-100 to remove the SDS, and the MMP activity was developed at 37 °C in the enzyme buffer (50 mM TrisHCl, 0.2 M NaCl, and 5 mM CaCl2, pH 7.5) for 24 h. After incubation, the gels were stained for 30 min in 0.125% Coomassie blue R-250 and the stain was removed with the same solution without the dye, until clear bands of gelatinolysis appeared on a dark background. Capillary whole blood gelatinases were used as a positive control. The MMP-2 and MMP-9 were identified by molecular size using high-molecular mass (14.5–200 kDa) standards (Bio-Rad, Hercules, CA). The images were processed and the intensity of the bands was obtained using the Gel Pro Analyzer (Media Cybernetics) image program.

TUNEL Assay

Cell death was examined by terminal deoxynucleotidyltransferase biotin dUTP nick end labeling (TUNEL) assay, (Roche, Mannheim, Germany) following the manufacturer's instructions. Retinal cell death was evaluated at P17 RA into three groups: noninjection, control IgG injection, and blocking antibody αIR3 injection. The slides were counterstained with methyl green to visualize the retinal layers. The slides were mounted with DPX Mounting Media (Sigma-Aldrich, St. Louis, MO). For each section, TUNEL-positive nuclei stained brown were counted from three randomly selected fields on either side of the optic nerve, and the average values from three separate sections, eye crossing the optic nerve, were combined to produce a mean value. The interval between each section was 15 mm apart. The field size of each picture was approximately 0.05 mm^2. The images were obtained under a light microscope (Nikon Eclipse TE2000-E, USA).

Statistical Treatment of Data

Results are presented as mean ± SEM or as median and interquartile range according to a parametric or nonparametric data distribution, respectively. When two datasets were compared, Mann–Whitney test was used to determine statistical significance according to a nonparametric data distribution. For multiple comparisons, one-way analysis of variance (ANOVA) was performed using Bonferroni post hoc test or Kruskal–Wallis with Dunn post hoc test, depending on a parametric or nonparametric data distribution. Statistical analyses were performed using the GraphPad Prism 5.0 software.

Results

Active MMP-2 Protein Expression Is Modified in Retinas of OIR Mice

Cellular migration and extracellular matrix (ECM) remodeling are key steps in pathological NV [21]. The MMPs (especially MMP-2 and MMP-9) are involved in this process, which is a hallmark of ROP and PDR [11, 17, 22–24]. The MMP-2 is secreted as a zymogen, pro MMP-2, whose activation requires the formation of a trimolecular complex with TIMP-2 and MT1-MMP [25]. For a more detailed understanding of MMP participation in the neovascular process, we evaluated the protein expression level of MMP-2 and MT1-MMP at critical time points of the OIR model.

As an evidence of the hypoxic treatments, VEGF protein levels increased and peaked at P17 (Fig. 1a, upper panel). Then, when we analyzed MMPs in neural retina extracts, we observed a similar expression pattern of MT1-MMP and MMP-2 from P12 to P20 OIR, with a significant increase at P17, which is in agreement with the peak of NV in the mouse model. In RA mice, MMP-2 protein level showed a gradual decrease as the retina matured, whereas MT1-MMP increased slightly at P17 (Fig. 1a). The quantitative analysis revealed a significant increase in the expression levels of both MMP-2 and MT1-MMP proteins at P17 OIR compared to P12 or P20 under the same condition. Moreover, even though the levels of

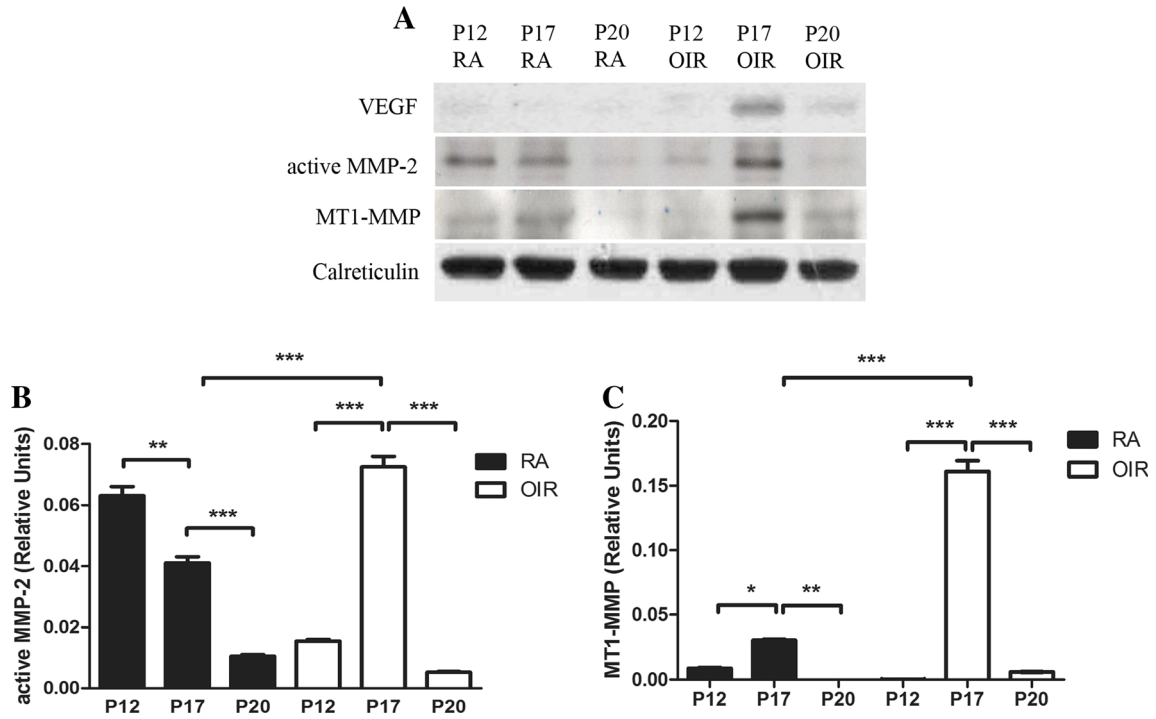

Fig. 1 Active MMP-2 protein expression is modified in retinas of OIR mice. **a** Representative Western blot assay of VEGF, active MMP-2, and MT1-MMP from neural retina extracts of RA and OIR mice at P12, P17, and P20. Calreticulin is shown as a loading control. **b** Levels of active MMP-2 and MT1-MMP were quantified and normalized by calreticulin. Data are presented as mean ± SEM. $*p < 0.05$; $**p < 0.01$; $***p < 0.001$. All the experiments were performed in triplicate and are representative of three independent experiments. $n = 3$ animals in each group

MMP-2 and MT1-MMP were high in P17 RA, the change of expression was much less pronounced than for OIR mice (Fig. 1b, c).

MMP-2 Modifies Its Localization Pattern in Neural Retina of OIR Mice Mainly at P17

Considering the results obtained by Western blot analysis related to MMP-2 expression, we next decided to investigate the retinal localization of this gelatinase in RA and OIR mice by immunohistochemical staining. The RA control retinas showed expression of MMP-2 mainly in the inner limiting membrane (ILM) and inner layers such as inner plexiform (IPL) and inner nuclear (INL) layers, but also in the OPL (Fig. 2, upper panel). This pattern of expression remained constant at different stages (P12, P17, and P20) of the retinal development. In the case of OIR mice, we observed an intense MMP-2 signal in the ILM at the three points evaluated and in the INL, mainly at P17 with respect to RA retinas (Fig. 2, upper panel). As evidenced by a double labeling, GS-positive cells were also positive for MMP-2, which confirmed the expression of MMP-2 by MGCs in RA and OIR retinas (Fig. 2, lower panel). Then, we focused on P17 (RA and OIR) retinas with the purpose of analyzing MMP-2 staining in the peak of NV. In RA mice, MMP-2 appears granular and distributed along the neural retina mainly at the end-feet of MGCs, being part of the ILM, and in the OPL (Fig. 3a, upper panel). In OIR mice, instead, the MMP-2 immunopositive signal was intensely observed also at the end-feet, in radial fibers spanning the entire retina and in the inner margin of the OPL. This possibly represents labeling of the so-called perisynaptic sheets of the MGCs, responsible for glutamate recycling at the ribbon synapses between photoreceptors and interneuron cells (Fig. 3a, lower panel). At this time, we also stained whole mount retinas with antibodies against MMP-2 and GS as well as GSA-IB4 lectin. The results revealed that, at P17, GS-positive cells were also positive for MMP-2 in both mice groups (Fig. 3b, upper and lower panels), which corroborated our previous results obtained in retinal cryosections. Finally, at higher magnifications, immunostaining at P17 OIR excluded expression of MMP-2 by neovessels and endothelial tip cells, which are vital for the development of new capillaries; however, an intense perivascular staining was observed in abnormal vessels in the superficial plexus (Fig. 3c). These results highlight the direct contribution of MMP-2 by MGCs during the neovascular phase of OIR.

The IGF-1R Changes Its Retinal Distribution, But Not Its Temporal Protein Level in OIR Mice Retinas

The OIR model provides an excellent opportunity to examine the role of hypoxia and hypoxia-regulated gene products (e.g., VEGF), as well as the contribution of other factors such as IGF-1, in the pathogenesis of retinal NV. There is strong

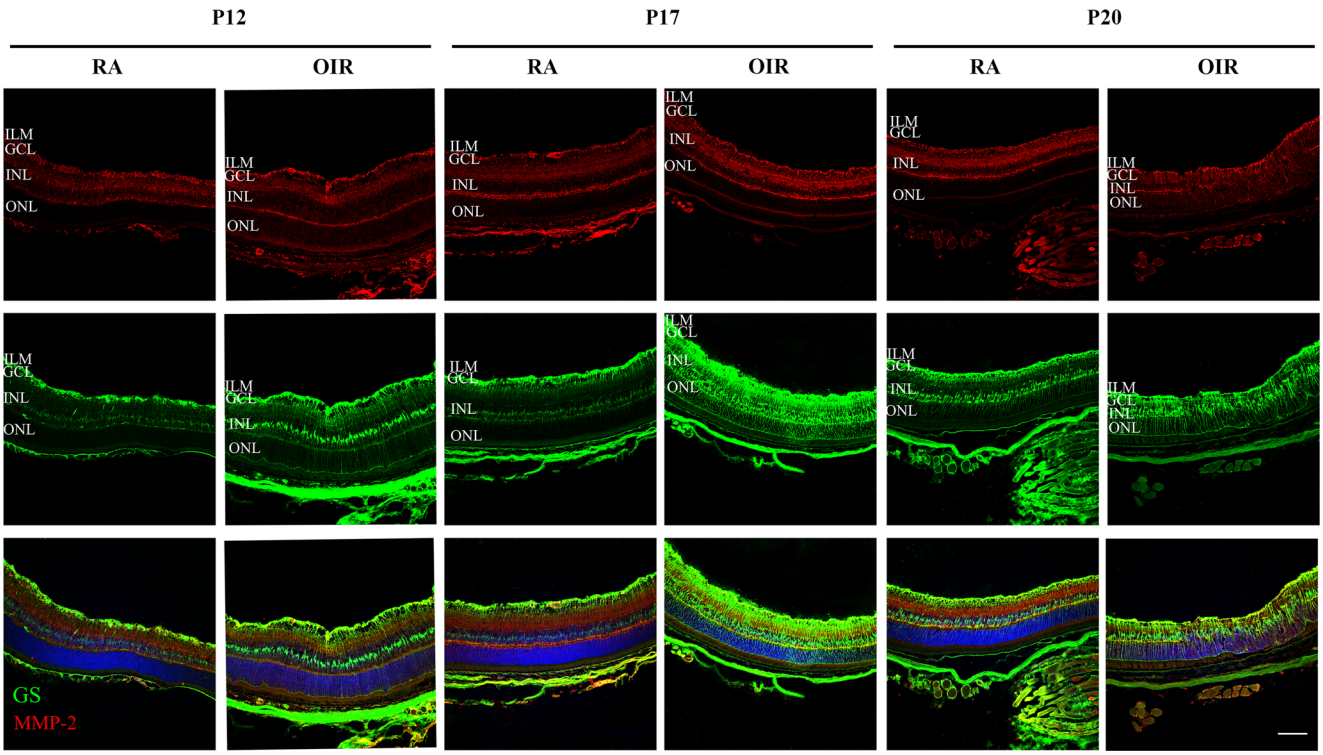

Fig. 2 MMP-2 modifies its localization pattern in neural retina of OIR mice mainly at P17. Representative immunofluorescence analysis of MMP-2 (*red*) in cryosections of RA and OIR mice retinas at P12, P17, and P20. The glial cell marker GS (*green*) highlights MGCs. Cell nuclei counterstained with Hoechst 33258 are also shown (*blue*). All the experiments were performed in triplicate and are representative of three independent experiments. $n = 3$ animals in each group. *ILM* inner limiting membrane, *GCL* ganglion cell layer, *INL* inner nuclear layer, *ONL* outer nuclear layer. *Scale bar*, 50 μm (color figure online)

evidence that IGF-1 and insulin receptors in retinal vascular endothelial cells are also relevant in normal and pathological angiogenesis [8, 26]. Here, with the purpose of analyzing the effect of the IGF-1/IGF-1R system on cells other than the endothelium, we examined the IGF-1R protein expression through the days and localization in OIR mice retinas. Figure 4a shows representative Western blot assays for IGF-1R at P12, P17, and P20 in RA and OIR mice. The quantitative analysis (Fig. 4b) revealed that the IGF-1R expression significantly increases at P17 in extracts of neural retinas in both RA and OIR mice, compared to all other time points analyzed under the same conditions. However, when the IGF-1R tissue expression was examined by immunofluorescence assays, we found changes in its localization in OIR neural retina with respect to RA mice (Fig. 4c). We observed that IGF-1R was expressed mainly in GCL and INL for RA mice, and faintly expressed in ONL at the different time points analyzed (Fig. 4c, upper panel). On the other hand, the IGF-1R expression at P12, P17, and P20 OIR in the retina was most prominent in areas adjacent to ILM, an area with great activity of neovessels, and to a much lesser extent in cells of the ONL (Fig. 4c, lower panel). This happened at the same time as the inner retina modified its structure and MGCs started their activation, which was confirmed by the GFAP positive staining. An increased degree of colocalization with GFAP was observed mainly in the region of the MGC end-feet for this period in OIR mice. These results indicate that although IGF-1R protein expression levels were maintained in the OIR mice compared with the RA control retinas, this receptor changed its retinal localization to GFAP positive cells, like MGCs, during the development of NV in the mouse OIR model.

The Intraocular Injection of Blocking Antibody αIR3 Ameliorates Pathological NV and Improves the Functionality of OIR Mice Retinas

Gelatin zymography assays were used to analyze the effect of hypoxia and the neovascular factors involved in the OIR model on the activity of MMPs at different periods of time. Retinal extracts of RA mice showed that MMP-2 during development is merely present as a pro MMP-2 form (72 kDa) together with lower levels of active MMP-2 form (62 kDa), mainly at P12 and P17. An increased activity of MMP-2 was observed in retinal extracts of OIR mice during the active phase of the neovascular process (Fig. 5a, b), which is in accordance with results previously obtained by Western blot assays.

In a previous study, we have shown that IGF-1 is able to regulate the extracellular level of MMP-2 activity in an in vitro model [14]. Thus, our next purpose was to analyze, in the OIR

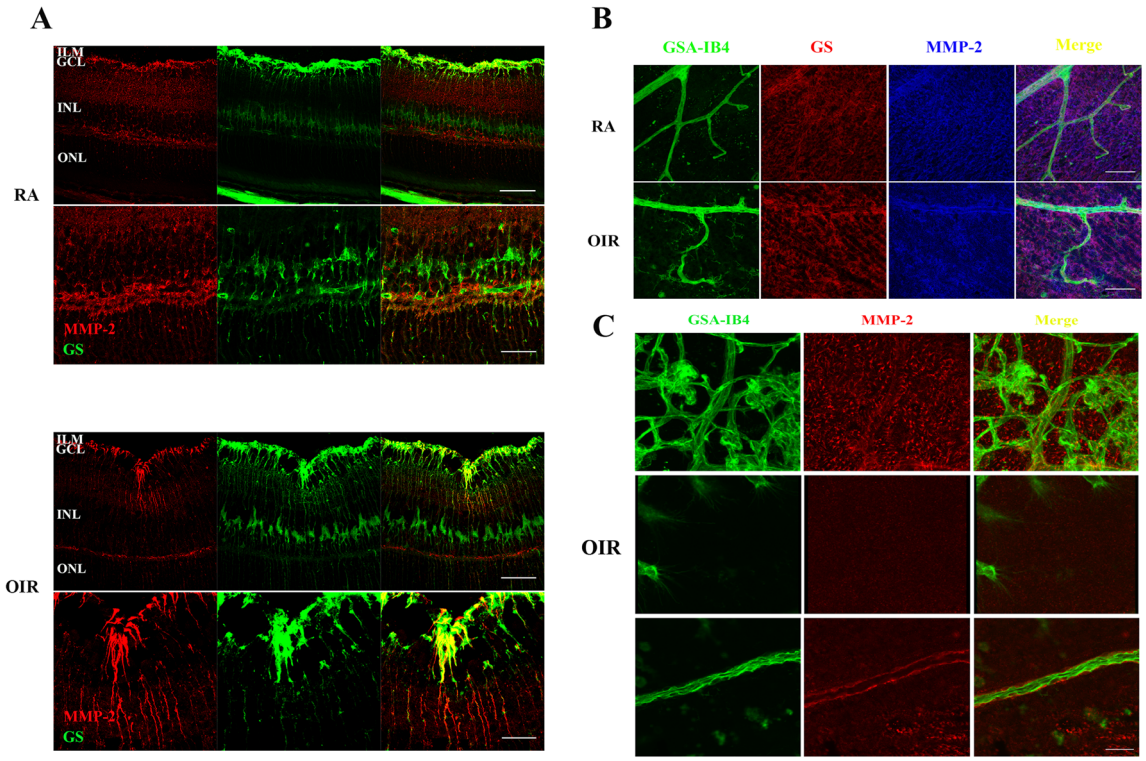

Fig. 3 MMP-2 is expressed by GS-positive cells. **a** Double labeling for MMP-2 (*red*) and MGCs marker GS (green) in representative cryosection of P17 RA mice retinas (upper panel) and in a magnified image showing the MGCs somata as well as in P17 OIR mice retinas (*lower panel*) and in a magnified image showing the MGCs end-feet and radial processes. **b** Triple labeling for MMP-2 (*blue*), GS (*red*), and GSA-IB4 (*green*) in the primary plexus on a P17 RA or OIR whole mount retinas. Note that GS distinguish MGCs from endothelium (GSA-IB4-positive cells). **c** High magnification confocal micrograph of the representative P17 OIR whole mount retina showing the neovascular area (*upper panel*), a typical filopodia extension at the leading edge of the primary retinal plexus (*middle panel*), and an aberrant primary retinal plexus (*lower panel*). All the experiments were performed in triplicate and are representative of three independent experiments. $n = 3$ animals in each group. *ILM* inner limiting membrane, *GCL* ganglion cell layer, *INL* inner nuclear layer, *ONL* outer nuclear layer. *Scale bar*, 50 μm (color figure online)

mice model, the MMP-2 activity regulation exerted by IGF-1R related to retinal vasculature and function. For this purpose, the blocking antibody αIR3, which specifically binds to the extracellular subunits of IGF-1R [27], was intravitreally injected at P12 in OIR mice. Considering that the effective dose to neutralize the IGF-1R signaling effect is 1 μg/mL in in vitro assays, we prepared a 100 μg/mL solution of the blocking antibody. Then, 1 μL of this solution or the nonspecific IgG (as control) was intravitreally injected. Pups from all groups were sacrificed on P17. Before injecting the OIR mice, we evaluated the effect of antibody αIR3 in P17 RA mice after administration at P12. The results clearly indicated that IgG or αIR3 injection did not alter the retinal structure (Supplementary Figure, A) or the vascular morphology (Supplementary Figure, B). TUNEL-positive cells were not observed, which demonstrated that the antibody itself or blocking IGF-1R does not interfere with retinal cell survival (Supplementary Figures, C). Figure 5c shows that a single intraocular injection of antibody αIR3 prevented vitreoretinal NV at P17 and accelerated revascularization of the central retina compared with IgG injected OIR mice (controls). Quantitative analysis revealed a 70% decrease of the avascular areas, whereas the retinal NV was reduced by 92% (Fig. 5d). Moreover, the decreased scotopic ERG retinal response observed in the IgG injected OIR eyes (controls) were attenuated by the blocking antibody αIR3 treatment. Whereas the average amplitudes of a- and b-wave were significantly recovery in the αIR3 injected eyes, a nonstatistical difference in the ERG a-wave and b-wave implicit time between IgG and αIR3 injected OIR eyes were observed (Fig. 5e).

Hypoxia Does Not Modify the IGF-1 Regulation of MMP-2 in MGCs

Considering the results obtained above, we decided to analyze the hypoxic effects on the MMP-2 regulation exerted by IGF-1 in MGCs mimicking the mouse OIR retinal environment. For this purpose, gelatin zymography was used to evaluate the extracellular levels of MMP-2 secreted by MIO-M1 cells stimulated with IGF-1 (8 h) under normoxia or hypoxia. As an evidence of the hypoxic treatments, we analyzed the protein expression of HIF-1α by Western blot assay (Fig. 6a, upper panel, b).

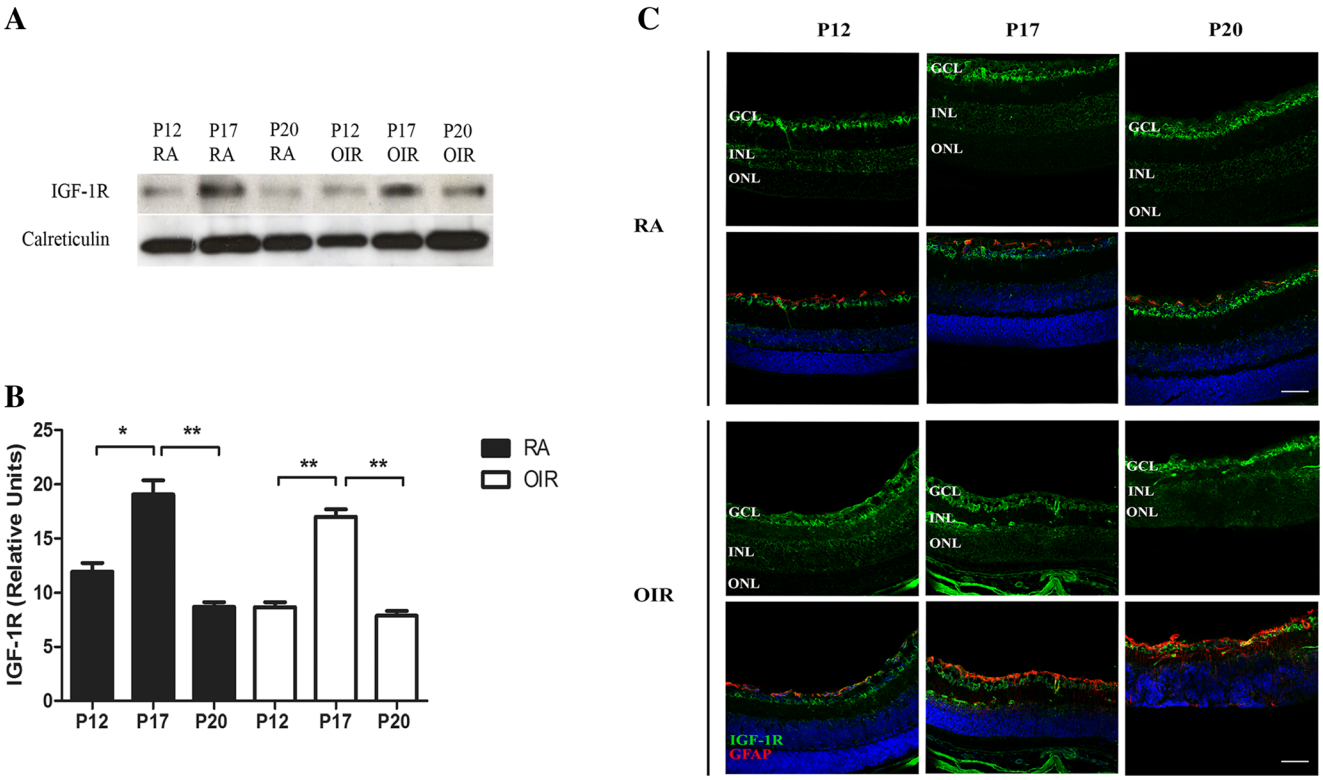

Fig. 4 The IGF-1R changes its retinal distribution, but not its temporal protein level in OIR mice retinas. **a** Representative Western blot assay of IGF-1R from neural retina extracts of RA and OIR mice at P12, P17, and P20. Calreticulin is shown as a loading control. **b** Levels of IGF-1R were quantified and normalized by calreticulin. Data are presented as mean ± SEM. *$p < 0.05$; **$p < 0.01$. **c** Representative immunofluorescence analysis of IGF-1R (*green*) in cryosections of RA (*upper panel*) and OIR (*lower panel*) mice retinas. The glial cell marker GFAP (*red*) highlights astrocyte and activated MGCs. Cell nuclei counterstained with Hoechst 33258 are also shown (*blue*). All the experiments were performed in triplicate and are representative of three independent experiments. $n = 3$ animals in each group. *GCL* ganglion cell layer, *INL* inner nuclear layer, *ONL* outer nuclear layer. *Scale bar*, 50 μm (color figure online)

Supernatants of normoxic and IGF-1-untreated MIO-M1 cells showed a constitutive expression of the pro MMP-2 together with a minor presence of the active MMP-2 form, which was significantly reduced after the IGF-1 treatment (Fig. 6a, lower panel, c). Under hypoxic conditions, the IGF-1 effect on active MMP-2 levels was similar to that observed under normoxic conditions. Then, MIO-M1 cells were cultured in the presence of antibody αIR3 to examine whether the effect of IGF-1 on the extracellular levels of active MMP-2 form was mediated by IGF-1R, independently of the normoxic or hypoxic conditions. The preincubation of MIO-M1 cells with blocking antibody abolish the IGF-1 effect on the active MMP-2 form without affecting the extracellular levels of pro MMP-2 form (Fig. 6a, lower panel, c). These results indicate that although the MMP-2/pro MMP-2 ratio increased under hypoxic conditions, the IGF-1 effect on MMP-2 was similar to the one previously demonstrated under normoxia [14], thus highlighting the key role of IGF-1 in the physiological and pathological processes involved in the regulation of MMP-2 extracellular proteolysis. Previous results demonstrated that, under these experimental conditions, pro- and active MMP-9 forms were undetectable and unaffected by the presence of IGF-1 [14].

Fig. 5 The intraocular injection of blocking antibody αIR3 ameliorates pathological NV and improves the functionality of OIR mice retinas. **a** Representative gelatin zymography of MMP-2 activity from retinal extracts samples of RA and OIR mice at P12, P17, and P20. Capillary whole blood gelatinases were used as a positive control. **b** In each case, bands corresponding to pro MMP-2 and active MMP-2 were quantified by densitometric analysis, and their ratios are represented in the *bar graphs* expressed in arbitrary units. Data are presented as mean ± SEM. *$p < 0.05$; **$p < 0.01$; ***$p < 0.001$. **c** Representative images of whole mount retinas at P17 showing GSA-IB4 staining in control IgG or αIR3 injected eyes. Avascular area and the area occupied by neovascularization tufts were outlined in *white* and *yellow*, respectively. **d** The avascular area (%) was quantified as the ratio of central avascular area to whole retinal area. Data are presented as median and interquartile range *$p < 0.05$. The neovascularization tufts area (%) was quantified as a percentage of whole retinal area. Data are presented as median and interquartile range *$p < 0.05$. **e** Average amplitudes and implicit times of scotopic ERG a-wave and b-wave recorded at P17 in RA and OIR eyes treated or not with αIR3 blocking antibody. Data are presented as median and interquartile range. *$p < 0.05$. All the experiments were performed in triplicate and are representative of three independent experiments. $n = 7$ animals in each group. *Scale bar*, 50 μm (color figure online)

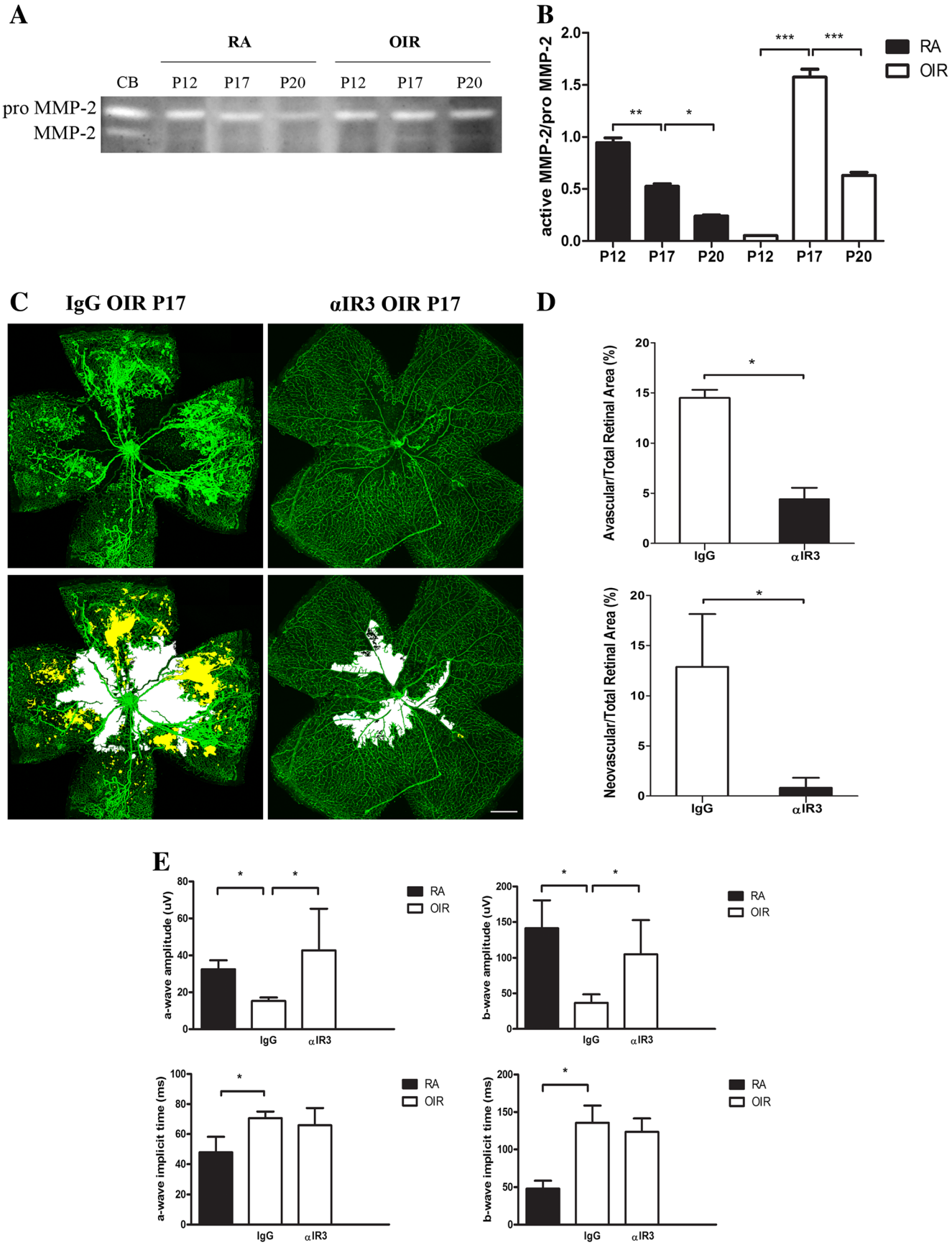
A
RA
OIR
CB
P12
P17
P20
P12
P17
P20
pro MMP-2
MMP-2
B
active MMP-2/pro MMP-2
RA
OIR
P12
P17
P20
P12
P17
P20
C
IgG OIR P17
αIR3 OIR P17
D
Avascular/Total Retinal Area (%)
IgG
αIR3
Neovascular/Total Retinal Area (%)
IgG
αIR3
E
a-wave amplitude (uV)
b-wave amplitude (uV)
a-wave implicit time (ms)
b-wave implicit time (ms)
RA
OIR
IgG
αIR3

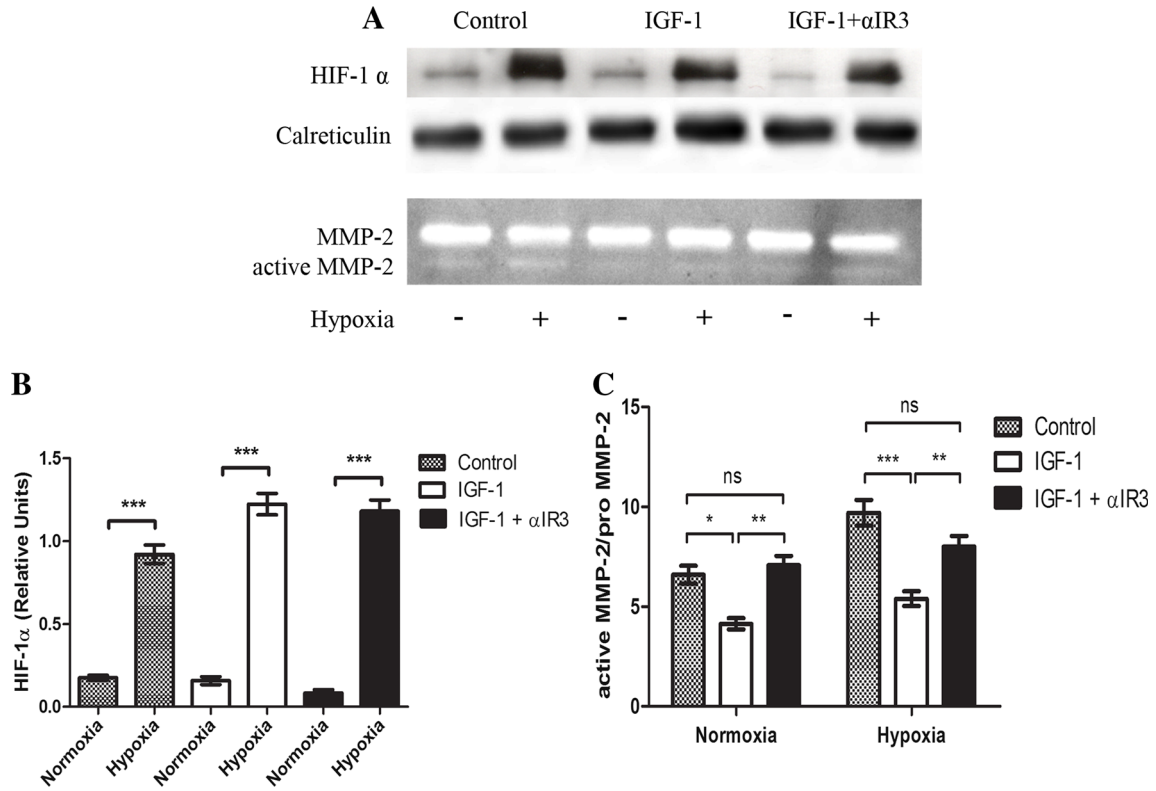

Fig. 6 Hypoxia does not modify the IGF-1 regulation of MMP-2 in MGCs. **a** Representative Western blot assay of HIF-1α from cell lysates of MIO-M1 cells exposed to normoxic or hypoxic conditions, pretreated with αIR3 antibody (16 nM) for 30 min and then stimulated with 10 nM IGF-1 for 8 h (*upper panel*). Calreticulin is shown as a loading control. Zymographic analysis of culture supernatants of MIO-M1 cells obtained under the same conditions of treatment (*lower panel*). **b** Levels of HIF-1α were quantified and normalized by calreticulin. **c** Pro MMP-2 and active MMP-2 were quantified by densitometric analysis, and their ratios were represented in the *bar graphs* and expressed in arbitrary units. Data are presented as mean ± SEM. *ns* nonsignificant. $*p < 0.05$; $**p < 0.01$; $***p < 0.001$. All the experiments were performed in triplicate and are representative of three independent experiments

Discussion

Degradation of ECM is an essential process in the development of vascular tissue. In the retina, the two major proposed events that may generate new vessels, angiogenesis and vasculogenesis, are dependent on proteases capable of cleaving the base membrane and ECM. The most significant proteases are matrix MMPs, a family of zinc-dependant endopeptidases with an extensive repertoire of substrates that include other proteases, growth factors, signaling molecules, cell surface receptors, and even intracellular targets. Among MMPs, MMP-2, and MMP-9 have been selectively associated with neovascular processes that occur in retinal pathologies like ROP and DR [11, 28–33]. Several laboratory studies focusing on NV have mainly considered the relation between endothelial cells and MMPs, highlighting their participation in cell migration and invasion during pathological angiogenesis. Nevertheless, MMPs are not only secreted by endothelial cells. In the retina, they have also been shown to be secreted by astrocytes [34, 35], human retinal pigment epithelial cells [36, 37], and MGCs. In the latter cells, basal MMP-2 expression has been described in healthy adult mice retinas [38], whereas both MMP-2 and MMP-9 have been expressed in culture of human MGCs [39]. We have demonstrated that IGF-1 regulates the extracellular level of active MMP-2 in human MGC line, MIO-M1 [14]. Our study emphasizes the significance of the in vitro findings by analyzing the retinal expression of MMP-2 in a mouse model of OIR. By Western blot assay, we demonstrate a peak in the expression of the active MMP-2 protein at P17. At the same time, MGCs were positive for MMP-2 at the end-feet area close to aberrant vessels. The gelatin zymography revealed that MMP-2 in retinal extracts at P17 was present in the active form. Moreover, the MT1-MMP expression was increased, thereby suggesting that relocalization of MMP-2 in areas adjacent to the vitreous humor cavity facilitates the conversion of pro MMP-2 into its active form, and that it enables the migration of endothelial and other cells such as MGCs, the retinal pigment epithelium (RPE) and fibroblasts during retinopathy. To our knowledge, the major contribution of this work is the demonstration of spatiotemporal changes in active MMP-2 protein expression during the NV as well as in retinal development. Recent publications have underlined the importance of using complementary sets of well-validated techniques to evaluate MMP

expression and activity [38]. Thus, in this work, we validate the MMP-2 results obtained by Western blot using gelatin zymography and show that the antibody selected was able to detect changes in the active form of this protease.

Retinal NV in the OIR model has been reported to be reduced in *Mmp-2* null mice by two groups [30, 31] but unaffected by other two [11, 35]. In addition, the formation of the retinal vascular plexus was not significantly different in MMP-2-deficient mice as compared to wild-type mice [29]. The significantly different levels of MMP-2 expression and activity observed in retinal extracts during development as well as in the OIR model may reflect the different roles exerted by this enzyme in normal physiological remodeling processes with respect to the course of NV. During vessel development, there was a tendency to reducing active MMP-2 expression levels according to vessel maturity. On the other hand, NV formation and regression are rapid processes in the OIR mouse model. We find a close association between the MMP-2 active levels at different stages of the OIR and the development of NV, which provides a clear picture of the role of MMP-2 in this process.

In addition to MMPs, IGF-1 has already been described as an angiogenic growth factor [40]. In humans, IGF-1 may act as a critical permissive factor for normal vascularization and neovascularization under circumstances when other angiogenic factors such as VEGF are expressed [7, 26]. Thus, IGF-1R mRNA is expressed over 100 times as much as insulin receptor (IR) during retinopathy, preferably in the INL where the MGCs bodies are located [10]. In this work, we were unable to show changes in the protein expression levels of IGF-1R during retinal development (RA) with respect to the OIR, which shows the lack of regulation under hypoxic conditions. Immunostaining of retinal cryosections demonstrated the colabeling for IGF-1R and GFAP during the NV phase in the OIR model. Moreover, IGF-1R modifies their distribution to P17 and it becomes more prominent towards the vitreous cavity, thus indicating that this receptor is actively involved during the peak of the NV. Previous studies have shown that knockout mice of insulin and IGF-1 receptors on vascular endothelial cells protect against retinal neovascularization [8, 41], which remarks the importance of the IGF-1/IGF-1R system during this process.

Considering that IGF-1R is also expressed by other retinal cells, we decided to analyze the effect of IGF-1 on the MMP-2 extracellular level regulation in the OIR mouse model. For this purpose, we intravitreally injected at P12 the monoclonal antibody αIR3, which specifically binds to the extracellular subunits of the IGF-1R [42]. This antibody has been widely used in the study of IGF-1R-mediated processes and IGF-1-mediated diseases such as cancer. About a hundred studies have been published on the investigation and therapeutic use of αIR3 with regard to its antitumor effect, administered either intraperitoneally (i.p.) or intravenously (i.v.) [43, 44], with the disadvantage that these routes of administration involve other tissues where this receptor is present. In this work, a single dose of αIR3 was intravitreally administered in the OIR mouse retina and selected according the following requirements: neutralizing dose recommended for in vitro studies, final concentration based on a mouse vitreal volume, and gradual degradation or inactivation of the antibody over time. Our results demonstrated that blocking IGF-1R effectively prevented the abnormal NV and it significantly enhanced the physiological revascularization of the retinal vascular plexus at P17, suggesting the in vivo regulation of MMP-2 active levels. In addition, it has been demonstrated that IGF-1R antagonism did not regulate VEGF or VEGF receptor expressions but rather reduced VEGF-induced MAPK activation in endothelial cells, which may also prevent NV exacerbation and promote a controlled retinal revascularization [5]. Finally, we identified sustained neuroretinal dysfunction in murine OIR, as demonstrated by reduced scotopic ERG responses, which was partially recovered after αIR3 administration.

In the retina, MGCs respond to hypoxia by stabilizing HIF-1α and secreting angiogenic cytokines such as VEGF [11]. At this time, we decided to analyze the effect of hypoxia on the regulation of MMP-2 exerted by IGF-1. The results showed that whereas the MMP-2/pro MMP-2 ratio increased under hypoxic conditions compared to normoxia, the IGF-1 effect on the extracellular levels of MMP-2 under hypoxia was similar to that shown under normoxia. A recent study has revealed that under hypoxic conditions (1% O_2), primary cultures of MGCs as well as MIO-M1 cells stabilize HIF-1 α, and thus promote activation of VEGF, which in endothelial cells increases the expression and activity of MMP-2 [11]. Our study demonstrated that, in addition to VEGF, IGF-1 is another growth factor strongly involved in NV, which is able to regulate the extracellular MMP-2 activity in MGCs, hence contributing to the MEC remodeling during this retinal process. In a previous study, we have demonstrated that an extracellular factor—activated α_2-macroglobulin (α_2M*)—which increases its level in the retina and vitreous humor in retinopathies, can induce the rapid MT1-MMP traffic to the plasma membrane through its receptor LRP1 in MGCs, and therefore promote MMP-2 activation [16]. The LRP1 integrates multiple signaling pathways and interacts with IGF-1R [45], strongly suggesting a putative mechanism through which it could modulate the levels of active MMP-2 under IGF-1 stimulus.

It is known that IGF-1exerts multiple effects on different retinal cell types under both physiological and pathological conditions. Despite the extensively described neuroprotective actions of the IGF-1, transgenic mice with increased intraocular levels of IGF-1 showed a progressive impairment of electroretinographic amplitudes up to a complete loss of response,

with loss of photoreceptors and bipolar, ganglion, and amacrine neurons. These results demonstrate that, when chronically increased, intraocular IGF-1 induces deleterious cellular processes that can lead to neurodegeneration. In this way, hypoxic retinas in the OIR mice model show higher levels of IGF-1 mRNA [46]. Hence, because upregulation and activation of proteases represent a final common pathway in the process of retinal NV, pharmacological intervention of this pathway may be an alternative therapeutic approach to proliferative retinopathy, where the blocking antibody αIR3 may play an important role not only by inhibiting the abnormal NV mediated by MMP-2, but also by the neurodegeneration induced by the elevated retinal levels of IGF-1.

Acknowledgements We thank Gabriela Diaz Cortez for her critical reading and language revision of the manuscript. We also thank Rosenstein laboratory for their help with ERG procedures, Carlos Mas, Maria Pilar Crespo and Cecilia Sampedro for confocal assistance, and Fabricio Navarro for animal care.

Compliance with Ethical Standards

Funding This study was funded by Secretaria de Ciencia y Tecnología-Universidad Nacional de Córdoba (SECyT-UNC) N° 203/14-103/15; Fondo para la Investigación Científica y Tecnológica (FONCyT), Préstamo BID 2008 PICT N° 1642, PICT 2012 N° 2607, and CONICET PIP 112-200801-02067.

Conflict of Interest The authors declare that they have no conflict of interest.

References

1. Scott A, Fruttiger M (2010) Oxygen-induced retinopathy: a model for vascular pathology in the retina. Eye (Lond) 24:416–421. doi:10.1038/eye.2009.306
2. Durham JT, Herman IM (2011) Microvascular modifications in diabetic retinopathy. Curr Diab Rep 11:253–264. doi:10.1007/s11892-011-0204-0
3. Casey R, Li WW (1997) Factors controlling ocular angiogenesis. Am J Ophthalmol 124:521–529
4. Ferrara N (2009) Vascular endothelial growth factor. Arterioscler Thromb Vasc Biol 29:789–791. doi:10.1161/ATVBAHA.108.179663
5. Smith LE, Shen W, Perruzzi C et al (1999) Regulation of vascular endothelial growth factor-dependent retinal neovascularization by insulin-like growth factor-1 receptor. NatMed 5:1390–1395. doi:10.1038/70963
6. Spranger J, Buhnen J, Jansen V et al (2000) Systemic levels contribute significantly to increased intraocular IGF-I, IGF-II and IGF-BP3 [correction of IFG-BP3] in proliferative diabetic retinopathy. Horm Metab Res = Horm und Stoffwechselforsch = Horm Metab 32:196–200. doi:10.1055/s-2007-978621
7. Hellstrom A, Perruzzi C, Ju M et al (2001) Low IGF-I suppresses VEGF-survival signaling in retinal endothelial cells: direct correlation with clinical retinopathy of prematurity. Proc Natl Acad Sci U S A 98:5804–5808. doi:10.1073/pnas.101113998
8. Kondo T, Vicent D, Suzuma K et al (2003) Knockout of insulin and IGF-1 receptors on vascular endothelial cells protects against retinal neovascularization. J Clin Invest 111:1835–1842. doi:10.1172/JCI17455
9. Burren CP, Berka JL, Edmondson SR et al (1996) Localization of mRNAs for insulin-like growth factor-I (IGF-I), IGF-I receptor, and IGF binding proteins in rat eye. Invest Ophthalmol Vis Sci 37:1459–1468
10. Lofqvist C, Willett KL, Aspegren O et al (2009) Quantification and localization of the IGF/insulin system expression in retinal blood vessels and neurons during oxygen-induced retinopathy in mice. Invest Ophthalmol Vis Sci 50:1831–1837. doi:10.1167/iovs.08-2903
11. Rodrigues M, Xin X, Jee K et al (2013) VEGF secreted by hypoxic Muller cells induces MMP-2 expression and activity in endothelial cells to promote retinal neovascularization in proliferative diabetic retinopathy. Diabetes 62:3863–3873. doi:10.2337/db13-0014
12. Sivak JM, Fini ME (2002) MMPs in the eye: emerging roles for matrix metalloproteinases in ocular physiology. Prog Retin Eye Res 21:1–14. doi:10.1016/S1350-9462(01)00015-5
13. Wride MA, Geatrell J, Guggenheim JA (2006) Proteases in eye development and disease. Birth Defects Res Part C Embryo Today Rev 78:90–105. doi:10.1002/bdrc.20063
14. Lorenc VE, Jaldín-Fincati JR, Luna JD et al (2015) IGF-1 regulates the extracellular level of active MMP-2 and promotes Müller glial cell motility. Invest Ophthalmol Vis Sci 56:6948–6960
15. Smith LE, Wesolowski E, McLellan A et al (1994) Oxygen-induced retinopathy in the mouse. Invest Ophthalmol Vis Sci 35:101–111
16. Barcelona PF, Jaldin-Fincati JR, Sanchez MC, Chiabrando GA (2013) Activated alpha2-macroglobulin induces Muller glial cell migration by regulating MT1-MMP activity through LRP1. FASEB J Off Publ Fed Am Soc Exp Biol 27:3181–3197. doi:10.1096/fj.12-221598
17. Sánchez MC, Luna JD, Barcelona PF et al (2007) Effect of retinal laser photocoagulation on the activity of metalloproteinases and the alpha(2)-macroglobulin proteolytic state in the vitreous of eyes with proliferative diabetic retinopathy. Exp Eye Res 85:644–650. doi:10.1016/j.exer.2007.07.018
18. Sanchez MC, Barcelona PF, Luna JD et al (2006) Low-density lipoprotein receptor-related protein-1 (LRP-1) expression in a rat model of oxygen-induced retinal neovascularization. Exp Eye Res 83:1378–1385. doi:10.1016/j.exer.2006.07.016
19. Limb GA, Salt TE, Munro PMG et al (2002) In vitro characterization of a spontaneously immortalized human Muller cell line (MIO-M1). Invest Ophthalmol Vis Sci 43:864–869
20. Kleiner DE, Stetler-Stevenson WG (1994) Quantitative zymography: detection of picogram quantities of gelatinases. Anal Biochem 218:325–329
21. van Hinsbergh VWM, Koolwijk P (2008) Endothelial sprouting and angiogenesis: matrix metalloproteinases in the lead. Cardiovasc Res 78:203–212. doi:10.1093/cvr/cvm102
22. Salzmann J, Limb GA, Khaw PT et al (2000) Matrix metalloproteinases and their natural inhibitors in fibrovascular membranes of proliferative diabetic retinopathy. Br J Ophthalmol 84:1091–1096
23. Webster L, Chignell AH, Limb GA (1999) Predominance of MMP-1 and MMP-2 in epiretinal and subretinal membranes of proliferative vitreoretinopathy. Exp Eye Res 68:91–98. doi:10.1006/exer.1998.0585
24. Noda K, Ishida S, Inoue M et al (2003) Production and activation of matrix metalloproteinase-2 in proliferative diabetic retinopathy. Invest Ophthalmol Vis Sci 44:2163–2170
25. Strongin a Y, Collier I, Bannikov G et al (1995) Mechanism of cell surface activation of 72-kDa type IV collagenase. J Biol Chem 270:5331–5338. doi:10.1074/jbc.270.10.5331
26. Hellström A, Carlsson B, Niklasson A et al (2002) IGF-I is critical for normal vascularization of the human retina. J Clin Endocrinol Metab 87:3413–3416. doi:10.1210/jcem.87.7.8629

27. Li YM, Schacher DH, Liu Q et al (1997) Regulation of myeloid growth and differentiation by the insulin-like growth factor I receptor. Endocrinology 138:362–368. doi:10.1210/endo.138.1.4847
28. Mohammad G, Kowluru R a (2011) Novel role of mitochondrial matrix metalloproteinase-2 in the development of diabetic retinopathy. Invest Ophthalmol Vis Sci 52:3832–3841. doi:10.1167/iovs.10-6368
29. Sarman S, van der Ploeg I, Seregard S, Kvanta A (2005) Retinal vascular development and pathologic retinal angiogenesis are not impaired in matrix metalloproteinase-2 deficient mice. Curr Eye Res 30:259–267. doi:10.1080/02713680590923212
30. Ohno-Matsui K, Uetama T, Yoshida T et al (2003) Reduced retinal angiogenesis in MMP-2-deficient mice. Invest Ophthalmol Vis Sci 44:5370–5375
31. Barnett JM, McCollum GW, Fowler JA et al (2007) Pharmacologic and genetic manipulation of MMP-2 and -9 affects retinal neovascularization in rodent models of OIR. Invest Ophthalmol Vis Sci 48:907–915. doi:10.1167/iovs.06-0082
32. Kowluru R a, Santos JM, Mishra M (2013) Epigenetic modifications and diabetic retinopathy. Biomed Res Int 2013:635284. doi:10.1155/2013/635284
33. Kowluru RA (2010) Role of matrix metalloproteinase-9 in the development of diabetic retinopathy and its regulation by H-Ras. Invest Ophthalmol Vis Sci 51:4320–4326. doi:10.1167/iovs.09-4851
34. He S, Prasanna G, Yorio T (2007) Endothelin-1-mediated signaling in the expression of matrix metalloproteinases and tissue inhibitors of metalloproteinases in astrocytes. Invest Ophthalmol Vis Sci 48:3737–3745. doi:10.1167/iovs.06-1138
35. Akhter N, Nix M, Abdul Y et al (2013) Delta-opioid receptors attenuate TNF-alpha-induced MMP-2 secretion from human ONH astrocytes. Invest Ophthalmol Vis Sci 54:6605–6611. doi:10.1167/iovs.13-12196
36. Dorecka M, Francuz T, Garczorz W et al (2014) The influence of elastin degradation products, glucose and atorvastatin on metalloproteinase-1, -2, -9 and tissue inhibitor of metalloproteinases-1, -2, -3 expression in human retinal pigment epithelial cells. Acta Biochim Pol 61:265–270
37. Marin-Castano ME, Csaky KG, Cousins SW (2005) Nonlethal oxidant injury to human retinal pigment epithelium cells causes cell membrane blebbing but decreased MMP-2 activity. Invest Ophthalmol Vis Sci 46:3331–3340. doi:10.1167/iovs.04-1224
38. De Groef L, Andries L, Lemmens K et al (2015) Matrix metalloproteinases in the mouse retina: a comparative study of expression patterns and MMP antibodies. BMC Ophthalmol 15:187. doi:10.1186/s12886-015-0176-y
39. Limb GA, Daniels JT, Pleass R et al (2002) Differential expression of matrix metalloproteinases 2 and 9 by glial Muller cells: response to soluble and extracellular matrix-bound tumor necrosis factor-alpha. Am J Pathol 160:1847–1855
40. Shaw LC, Grant MB (2004) Insulin like growth factor-1 and insulin-like growth factor binding proteins: their possible roles in both maintaining normal retinal vascular function and in promoting retinal pathology. Rev Endocr Metab Disord 5:199–207. doi:10.1023/B:REMD.0000032408.18015.b1
41. Shaw LC, Pan H, Afzal A et al (2006) Proliferating endothelial cell-specific expression of IGF-I receptor ribozyme inhibits retinal neovascularization. Gene Ther 13:752–760. doi:10.1038/sj.gt.3302718
42. Kull FCJ, Jacobs S, Su YF et al (1983) Monoclonal antibodies to receptors for insulin and somatomedin-C. J Biol Chem 258:6561–6566
43. Rohlik QT, Adams D, Kull FCJ, Jacobs S (1987) An antibody to the receptor for insulin-like growth factor I inhibits the growth of MCF-7 cells in tissue culture. Biochem Biophys Res Commun 149:276–281
44. Adams TE, Epa VC, Garrett TP, Ward CW (2000) Structure and function of the type 1 insulin-like growth factor receptor. Cell Mol Life Sci 57:1050–1093. doi:10.1007/PL00000744
45. Woldt E, Matz RL, Terrand J et al (2011) Differential signaling by adaptor molecules LRP1 and ShcA regulates adipogenesis by the insulin-like growth factor-1 receptor. J Biol Chem 286:16775–16782. doi:10.1074/jbc.M110.212878
46. Ristori C, Filippi L, dal Monte M et al (2011) Role of the adrenergic system in a mouse model of oxygen-induced retinopathy: Antiangiogenic effects of β-adrenoreceptor blockade. Investig Ophthalmol Vis Sci 52:155–170. doi:10.1167/iovs.10-5536